Spin state and magnetic transformations in $Sr_{0.7}Y_{0.3}CoO_{2.62}$ at high pressures

N. O. Golosova,[1] D. P. Kozlenko,[1] L. S. Dubrovinsky,[2] O. A. Drozhzhin,[3] S. Ya. Istomin,[3] and B. N. Savenko[1]
[1]*Frank Laboratory of Neutron Physics, JINR, 141980 Dubna, Russia*
[2]*Bayerisches Geoinstitut, Universität Bayreuth, Bayreuth D-95440, Germany*
[3]*Department of Chemistry, Moscow State University, 119992 Moscow, Russia*
(Received 4 February 2009; published 27 March 2009)

The crystal and magnetic structures of $Sr_{0.7}Y_{0.3}CoO_{2.62}$ were studied at high pressures up to 30 and 5 GPa by means of x-ray and neutron diffraction, respectively. An evidence for the pressure-induced change in the spin state of Co^{3+} ions in octahedral coordination from intermediate spin to low spin was found from a behavior of Co-O bond lengths and obtained ordered magnetic moments values. The high spin state of the tetrahedral and five-coordinated Co^{3+} ions in oxygen deficient layers remains stable under pressure. A rapid suppression of the initial *G*-type antiferromagnetic (AFM) state and a formation of the new AFM state with a propagation vector (1/2 1/2 1) was found. The possible mechanisms of the pressure-induced magnetic transformation are discussed.

DOI: 10.1103/PhysRevB.79.104431 PACS number(s): 75.25.+z, 61.50.Ks, 71.30.+h

I. INTRODUCTION

The cobalt-oxide-based materials exhibit spectacular phenomena which are extensively studied at present time—giant magnetoresistance, insulator-metal transition, orbital and charge ordering, and variable magnetic structures.[1–8] The unique feature of cobalt oxides, making them distinctive from manganites or cuprates, is a spin degree of freedom of Co^{3+} ions. Depending on the delicate balance of comparable values of intra-atomic exchange energy (J_H) and crystal-field splitting (Δ_{CF}), low spin (LS) ($t_{2g}^6, S=0$), intermediate spin (IS) ($t_{2g}^5 e_g^1, S=1$), or high spin (HS) ($t_{2g}^4 e_g^2, S=2$) states can be realized.[1,9–12]

In perovskitelike cobaltites $RCoO_3$ (*R* as rare-earth element) a thermally induced LS-IS/HS crossover leads to a change in the ground state from low-temperature nonmagnetic to high-temperature paramagnetic at $T \approx 100-800$ K (R=La-Y), followed by the semiconductor-metal phase transition at $T=500-820$ K (La-Y).[1,9–13] Upon substitution of rare-earth *R* by alkali earth *A* element, a ferromagnetic (FM) ground state is stabilized in $R_{1-x}A_xCoO_3$ compounds for $x > 0.18$.[2,14]

More intriguing and complex physical properties were found in related oxygen-deficient cobalt oxides $RBaCo_2O_{5+d}$ with ordering of R/Ba cations and oxygen vacancies, which exhibit correlating spin state and insulator-metal transitions, spin state ordering and giant magnetoresistance due to competition between ferromagnetic and antiferromagnetic orderings.[3–8] The crystal structure of these compounds contains alternating oxygen-rich CoO_6 octahedral and oxygen-deficient CoO_5 pyramidal layers. Although it is generally considered that the insulator-metal transition in $RBaCo_2O_{5+d}$ ($d \sim 0.5$) is caused by a spin state change of Co^{3+} ions in CoO_6 octahedra, its mechanism is still controversial and extensively debated. Proposed scenarios involve full or partial LS-IS or LS-HS spin state transition for octahedrally coordinated Co^{3+} ions and IS or HS spin configuration for Co^{3+} ions in pyramidal coordination.[6–8,15–17]

Recently a novel class of relevant oxygen deficient cobalt oxides $R_{1-x}Sr_xCoO_{3-d}$ (R=Y, Ho, Gd, and Dy, $x \sim 0.7$, and $d \sim 0.2-0.4$) was synthesized.[18–23] These compounds crystallize in the brownmilleritelike tetragonal structural phase (314 phase) with $I4/mmm$ symmetry and lattice parameters $a \approx 2a_p$ and $c \approx 4a_p$ (a_p: lattice parameter of ideal perovskite subcell). It consists of layers formed by Co atoms in octahedral coordination of oxygen atoms which alternate with oxygen-deficient layers formed by Co atoms in tetrahedral and five-coordinated oxygen surroundings. The physical properties of $R_{1-x}Sr_xCoO_{3-d}$ ($x \sim 0.7, d \sim 0.2-0.4$) are less studied but some similarity with $RBaCo_2O_{5+d}$ can be found despite structural difference. These compounds exhibit the *G*-type antiferromagnetic (AFM) ground state,[18–23] and similar AFM states are also observed in $RBaCo_2O_{5+d}$.[6,7,16,17] In $Sr_{2/3}Y_{1/3}CoO_{3-d}$ the insulator-metal transition occurs upon increase in oxygen content from $3-d=2.66-2.70$.[24] The magnetization jump associated with a spin state transition of Co^{3+} was found in $Sr_{0.67}Y_{0.33}CoO_{2.614}$ and $Sr_{0.67}Y_{0.33}CoO_{2.704}$.[25]

A complexity and drastic modification of physical properties of oxygen deficient cobalt oxides in comparison with stoichiometric ones imply a crucial role of a specific geometry of oxygen coordination and its sharp effect on the Co^{3+} ion spin states equilibria upon variation in interatomic distances. A crucial insight into the formation of magnetic properties of layered oxygen deficient cobalt oxides and their relationship with a stability of different spin states of Co^{3+} ions can be obtained from a study of crystal and magnetic structures at high pressure. It provides an opportunity to study a response of magnetic structure and Co^{3+} spin state upon variation in structural parameters and Co-O bond lengths.

In this paper, crystal and magnetic structures of oxygen deficient $Sr_{0.7}Y_{0.3}CoO_{2.62}$ compound, containing mostly Co^{3+} ions (94%), was studied by means of x-ray and neutron powder diffraction at high pressures up to 30 and 5 GPa, respectively.

II. EXPERIMENTAL

The compound $Sr_{0.7}Y_{0.3}CoO_{2.62}$ was synthesized from stoichiometric mixtures of $SrCO_3$, Co_3O_4, and Y_2O_3. The

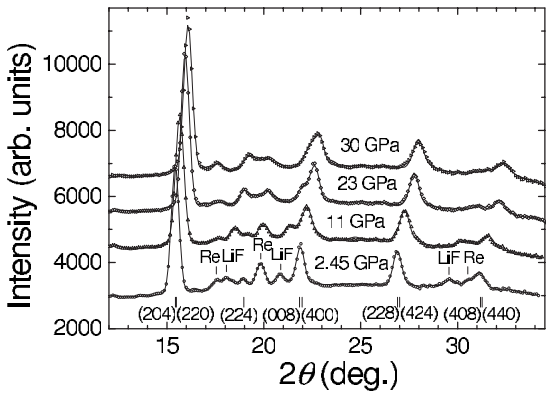

FIG. 1. X-ray diffraction patterns of $Sr_{0.7}Y_{0.3}CoO_{2.62}$ measured at selected pressures and ambient temperature and processed by the Rietveld method. Experimental points and calculated profiles are shown. The most intense reflections indices are shown by vertical line marks at the bottom. Positions of diffraction peaks from the pressure transmitting medium (LiF) and gasket (Re) are marked.

mixtures were carefully ground and sintered in air at 1423 K for 24 h, followed by a regrinding and further firing at 1423 K for 72 h. Thereafter, the furnace was shut off and the samples were allowed to cool to room temperature.

X-ray powder-diffraction measurements were made at high pressures up to 30 GPa and ambient temperature with a diamond-anvil cell.[26] The sample was loaded in the Re gasket with LiF powder as a pressure transmitting medium, admixed in proportion 2:1. The pressure was measured using the ruby fluorescence technique. The x-ray diffraction (XRD) spectra were measured at the system consistent of high-brilliance FRD rotating anode generator (Mo $K\alpha$ radiation, $\lambda=0.7115$ Å), FluxMax focusing optics, and Bruker APEX charge coupled device (CCD) area detector. The two-dimensional XRD images were converted to conventional one-dimensional diffraction patterns using FIT2D program.[27] The data analysis was performed using GSAS program.[28]

Neutron powder-diffraction measurements at high pressures up to 5 GPa were performed at selected temperatures in the range 10–290 K with the DN-12 spectrometer[29] at the IBR-2 high-flux pulsed reactor (FLNP JINR, Dubna, Russia) using the sapphire anvil high-pressure cells.[30] Diffraction patterns were collected at scattering angles 45.5° and 90° with the resolution $\Delta d/d=0.022$ and 0.015, respectively. Experimental data were analyzed by the Rietveld method using MRIA program[31] or FULLPROF (Ref. 32) if magnetic structure was to be included.

III. RESULTS AND DISCUSSION

X-ray diffraction patterns of $Sr_{0.7}Y_{0.3}CoO_{2.62}$ obtained at selected pressures and ambient temperature and processed by the Rietveld method are shown in Fig. 1. The tetragonal crystal structure[18] of $I4/mmm$ symmetry remains stable in the investigated pressure range up to 30 GPa. The lattice compression is slightly anisotropic with an increase in $c/2a$ lattice parameters ratio (Fig. 2). The unit-cell volume as a function of pressure was fitted by the Birch-Murnaghan equation of state:[33]

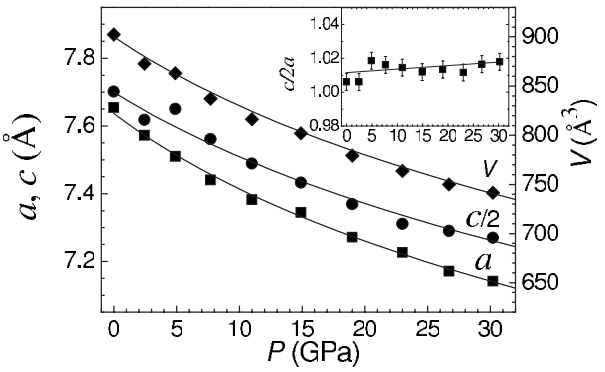

FIG. 2. Lattice parameters, their ratio (inset), and unit-cell volume of $Sr_{0.7}Y_{0.3}CoO_{2.62}$ as functions of pressure. The estimated error bars for lattice parameters and unit-cell volume are within symbol sizes.

$$P=\frac{3}{2}B_0(x^{-7/3}-x^{-5/3})\left[1+\frac{3}{4}(B'-4)(x^{-2/3}-1)\right],$$

where $x=V/V_0$ is the relative volume change, V_0 is the unit-cell volume at $P=0$, and B_0 and B' are the bulk modulus $[B_0=-V(dP/dV)_T]$ and its pressure derivative $[B'=(dB_0/dP)_T]$. The calculated value $B_0=105(5)$ GPa with fixed $B'=4$ and experimental value of $V_0=902.5(7)$ Å^3 is considerably smaller than ones $B_0=146$ and 158 GPa for relevant stoichiometric compounds $La_{0.7}Sr_{0.3}CoO_3$ and $La_{0.82}Sr_{0.18}CoO_3$, respectively.[34,35] A decrease in the bulk modulus in $Sr_{0.7}Y_{0.3}CoO_{2.62}$ can be related to a presence of oxygen vacancies, effectively reducing the atomic density in comparison with stoichiometric compounds.

The characteristic neutron-diffraction patterns of $Sr_{0.7}Y_{0.3}CoO_{2.62}$ measured at selected pressures and $T=10$ K are shown in Fig. 3. The structural parameters obtained from Rietveld refinement of diffraction data at se-

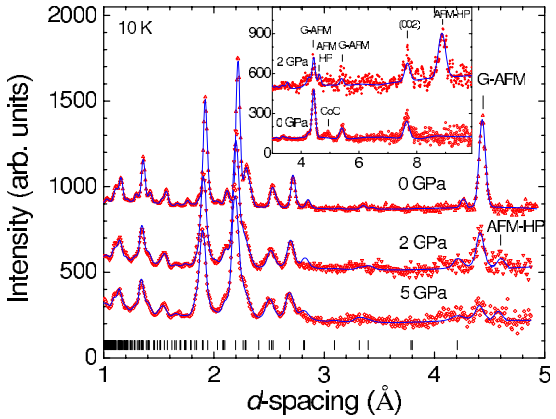

FIG. 3. (Color online) Neutron-diffraction patterns of $Sr_{0.7}Y_{0.3}CoO_{2.62}$ measured at different pressures and temperatures and processed by the Rietveld method. Ticks below represent calculated positions of nuclear peaks. The most intense magnetic peaks from initial G-type AFM phase and pressure-induced AFM phase are marked as "G-AFM" and "AFM-HP," respectively. The position of magnetic peak from CoO impurity, found in amount of about 4% in the sample, is also shown.

TABLE I. Structural parameters of $Sr_{0.7}Y_{0.3}CoO_{2.62}$ at selected pressures and ambient temperature obtained from neutron diffraction experiment. The atomic positions are: Sr1/Y1—4(e) (0,0,z), Sr2/Y2—8(g) (0,0.5,z), Sr3/Y3—4(e) (0,0,z), Co1—8(h) (x,x,0), Co2—8(f) (0.25, 0.75, 0.25), O1—16(n) (0,y,z), O2—16(m) (x,x,z), O3—8(i) (0,y,0), and O4—8(j) (x,0.5,0) of the space group $I4/mmm$. The occupation of the O4 position is 1/4.

P (GPa)	0	2.0	5.0
a (Å)	7.630(3)	7.566(4)	7.504(4)
b (Å)	15.294(5)	15.273(6)	15.203(6)
Sr1/Y1:z	0.869(2)	0.863(3)	0.869(3)
Sr2/Y2:z	0.875(2)	0.866(3)	0.862(3)
Sr3/Y2:z	0.341(2)	0.335(3)	0.335(3)
Co1:x	0.752(3)	0.750(4)	0.746(4)
O1:y	0.256(3)	0.255(5)	0.252(5)
z	0.242(3)	0.245(5)	0.243(5)
O2:x	0.289(3)	0.284(4)	0.284(4)
z	0.116(2)	0.122(4)	0.122(4)
O3:y	0.749(2)	0.746(5)	0.746(5)
O4:x	0.380(2)	0.379(3)	0.380(3)
R_p (%)	7.90	7.03	7.30
R_{wp} (%)	4.50	5.51	5.68

lected pressures and ambient temperature are listed in Table I. At ambient pressure their values are close to ones previously reported.[18] Below $T_N \approx 335$ K at ambient pressure an appearance of magnetic lines (1 1 2) at 4.4 and (1 1 0) at 5.4 Å (marked as G-AFM in Fig. 3), characteristic for the onset of the G-type AFM state [Fig. 4(b)] was observed. The nonzero intensity of the (1 1 0) peak originates from different ordered magnetic moments values of Co1 and Co2 ions, located in oxygen-deficient and octahedrally coordinated layers, respectively.[36] The obtained values $\mu_{Co1}=3.0(1)\mu_B$ and $\mu_{Co2}=1.3(1)\mu_B$ at $T=10$ K imply the HS ($S=2$) and IS ($S=1$) states of Co^{3+} ions located at Co1 and Co2 positions. The elongation of the CoO_6 octahedra along the c axis, having apical bond lengths $l_{Co2\text{-}O2}=2.089(5)$ Å much larger than those $l_{Co2\text{-}O1}=1.911(5)$ Å lying in (ab) planes, supports the IS state nature of Co2 ions with the $d(3z^2-r^2)$ e_g orbital polarization. Simultaneously, the CoO_4 tetrahedra in oxygen deficient layers are compressed along the c axis with the bond lengths $l_{Co1\text{-}O2}=1.825(5)$ Å much smaller than those $l_{Co1\text{-}O3}=1.891(5)$ Å lying in (ab) planes. Due to a presence of an additional oxygen atom disordered over four equivalent and closely located positions with occupancy of 0.25, there is an additional in-plane bond with a length of $l_{Co1\text{-}O4}=2.144(5)$ Å.

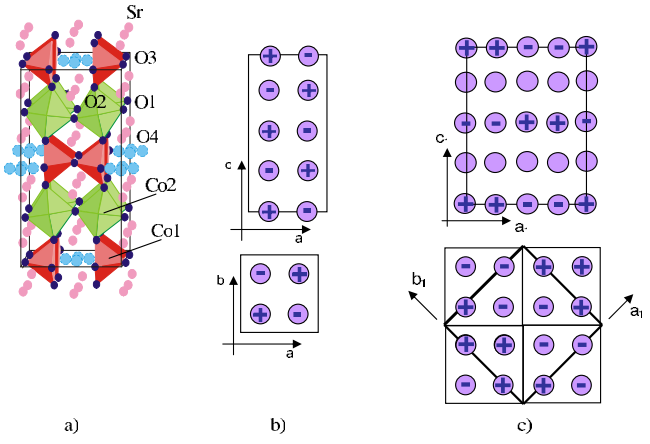

FIG. 4. (Color online) Crystal structure of $Sr_{0.7}Y_{0.3}CoO_{2.62}$ with a tetragonal $I4/mmm$ symmetry (a). Co atoms are located inside tetrahedra and octahedra formed by oxygen atoms. Magnetic structures of $Sr_{0.7}Y_{0.3}CoO_{2.62}$ at (b) ambient and (c) high pressures, shown as projections on (ac) and (ab) planes. Signs (+) and (–) denote relevant directions of Co ordered magnetic moments, oriented along the c axis in the G-type AFM state and located in the (ab) planes for the pressure-induced AFM state. Empty circles correspond to Co^{3+} ions with the LS state.

At high pressures $P \geq 2$ GPa a rapid decrease in the intensity of magnetic peaks corresponding to the G-type AFM state was observed. Simultaneously, below $T_{N1} \approx 250$ K an appearance of additional magnetic peaks (1/2 0 1)(0 1/2 1) at 8.89 Å and (1/2 0 3)(0 1/2 3) at 4.62 Å was detected (marked as AFM-HP in Fig. 3). They correspond to a formation of the new AFM state with a propagation vector $k=(1/2\ 1/2\ 1)$ and can be indexed in the magnetic cell with lattice parameters $a\sqrt{2}$, $a\sqrt{2}$, and c. From the analysis by the Rietveld method it was found that in the pressure induced AFM state (AFM-HP) Co^{3+} magnetic moments form ferromagnetic chains oriented along (100) directions with FM-FM-AFM-AFM coupling between adjacent chains (Fig. 4). For a comparison, the relative magnetic coupling in the initial G-type AFM state is FM-AFM-FM-AFM (Fig. 4). The magnetic coupling between adjacent oxygen-deficient layers along the c axis in the AFM-HP state is AFM, while it was FM in the initial G-type AFM state. The obtained magnetic-moment values at $P=2$ GPa and $T=10$ K are $\mu_{Co1}=3.0(2)\mu_B$ and $\mu_{Co2}=0.5(2)\mu_B$ at $T=10$ K. A very small value of the ordered magnetic moment for Co^{3+} ions in octahedral coordination provides evidence for the pressure-induced change of the spin state from IS to LS ($S=0$), while HS spin state of Co^{3+} ions in tetrahedral and five-coordinated oxygen surroundings remain stable under pressure. The volume ratio of the suppressed G-type AFM state and newly appeared AFM-HP phases increases from 0.5:0.5 at 2 GPa to 0.2:0.8 at 5 GPa and 10 K.

It is interesting to note that spin-state-ordered arrangements of somewhat different geometry were observed in related oxygen-deficient $RBaCo_2O_{5.5+d}$ compounds, involving formation of LS state of Co^{3+} ions in octahedral coordination and HS (or IS) state of Co^{3+} ions in pyramidal coordination at ambient pressure and low temperature.[3–8] A gradual pressure-induced suppression of the IS spin state with respect to LS one for Co^{3+} ions in octahedral coordination was also previously found for perovskitelike stoichiometric compounds $LaCoO_3$ (Ref. 12) and $R_{1-x}A_xCoO_3$ (Ref. 34) although it is less pronounced than in the case of $Sr_{0.7}Y_{0.3}CoO_{2.62}$.

The pressure dependences of Co-O bond lengths demonstrate specific behavior in the vicinity of $P_{tr}=2$ GPa (Fig. 5), corresponding to the magnetic and spin state transitions in $Sr_{0.7}Y_{0.3}CoO_{2.62}$. In CoO_6 octahedra, the longest apical bond

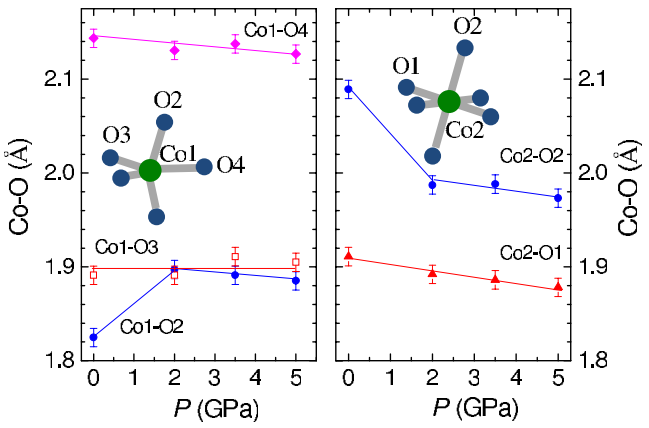

FIG. 5. (Color online) Co-O distances as functions of pressures in oxygen-deficient layers (left) and layers with octahedral oxygen coordination (right) of $Sr_{0.7}Y_{0.3}CoO_{2.62}$ at ambient temperature. The lines are guides to eyes only.

length shortens rapidly from $l_{Co2\text{-}O2}=2.089(5)$ to 1.987(8) Å in 0–2 GPa pressure range, while with a further pressure increase it decreases slightly to 1.973(8) Å at $P=5$ GPa. The in-plane bond length decreases smoothly from 1.911(5) to 1.878(8) Å in 0–5 GPa pressure range (Fig. 5). As a result, CoO_6 octahedra become more isotropic at high pressures, which is expectable for the IS-LS spin state modification, leading to a depopulation of polarized e_g orbitals.[9–13] In CoO_4 tetrahedra, the apical bond length increases from $l_{Co1\text{-}O2}=1.825(5)-1.878(8)$ Å in 0–2 GPa pressure range and it decreases to 1.885(8) Å with a further pressure increase up to 5 GPa (Fig. 5). Such a behavior is caused by the apical oxygen O2 shift toward Co2 ion due to IS-LS spin state transition. The in-plane bond length remains about the same within the determination accuracy, $l_{Co1\text{-}O3} \approx 1.900(8)$ Å, while an additional bond length with a disordered oxygen decreases from $l_{Co1\text{-}O4}=2.144(5)-2.127(8)$ Å in 0–5 GPa pressure range. The Co2-Co2 and Co1-Co1 distances decrease under pressure, following the behavior of lattice parameters (Fig. 2) without any peculiarities.

The observed pressure-induced magnetic transformation in $Sr_{0.7}Y_{0.3}CoO_{2.62}$ can be related to a modification of the balance of magnetic interactions between Co1 ions in oxygen deficient layers. In the *c*-axis direction, the Co1(HS)-O2-Co2(LS)-O2-Co1(HS) AFM superexchange interactions are formed due to spin state change of Co2 ions in octahedral layers. Within the oxygen deficient layers, the Co1-O3-Co1 superexchange interactions have AFM character, while there are competing magnetic superexchange Co1-O4-Co1 and direct exchange Co1-Co1, expected to be of FM nature, due to a disorder of the only one O4 oxygen over four equivalent positions (Fig. 6). A pressure tuning of the balance between these competing interactions can also be expected to induce changes in the magnetic ground state.

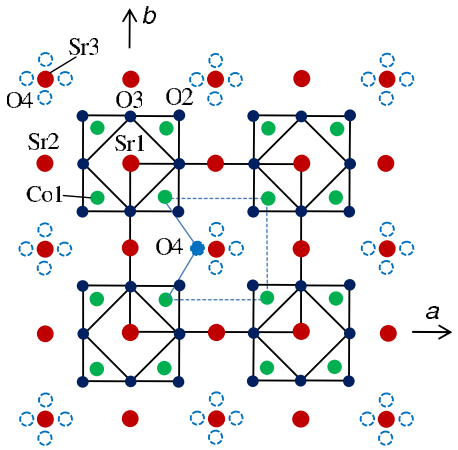

FIG. 6. (Color online) Structural arrangement of oxygen deficient layers ($z=0.0$) in the crystal structure of $Sr_{0.7}Y_{0.3}CoO_{2.62}$. One O4 oxygen atom is disordered over four equivalent positions. It leads to a presence of AFM superexchange Co1-O4-Co1 and FM direct exchange Co1-Co1 competing interactions, which are schematically illustrated as light blue (gray) solid and dash lines.

IV. CONCLUSIONS

Our results demonstrate that in $Sr_{0.7}Y_{0.3}CoO_{2.62}$ the spin state of Co^{3+} ions in octahedral coordination is remarkably unstable at high pressures and it changes from IS to LS, while the HS state of Co^{3+} ions in tetrahedral and five-coordinated oxygen surroundings in oxygen deficient layers remains stable upon compression. This pressure-induced spin state modification and competing character of superexchange and direct exchange magnetic interactions between Co^{3+} ions in oxygen deficient layers result in the instability of the initial *G*-type AFM magnetic state and lead to a formation of the AFM magnetic state with a propagation vector $k=(1/2\ 1/2\ 1)$.

ACKNOWLEDGMENTS

The work was supported by the RFBR under Grant No. 08-02-90018-Bel-a and BRFFR-JINR under Grant No. H08D-002. The financial support from BGI is also gratefully acknowledged.

[1] P. M. Raccah and J. B. Goodenough, Phys. Rev. **155**, 932 (1967).
[2] M. A. Señarís-Rodríguez and J. B. Goodenough, J. Solid State Chem. **118**, 323 (1995).
[3] C. Martin, A. Maignan, D. Pelloquin, N. Nguyen, and B. Raveau, Appl. Phys. Lett. **71**, 1421 (1997).
[4] I. O. Troyanchuk, N. V. Kasper, D. D. Khalyavin, H. Szymczak, R. Szymczak, and M. Baran, Phys. Rev. Lett. **80**, 3380 (1998).
[5] T. Vogt, P. M. Woodward, P. Karen, B. A. Hunter, P. Henning, and A. R. Moodenbaugh, Phys. Rev. Lett. **84**, 2969 (2000).

[6] C. Frontera, J. L. Garcia-Munoz, A. Llobet, and M. A. G. Aranda, Phys. Rev. B **65**, 180405(R) (2002).
[7] A. A. Taskin, A. N. Lavrov, and Y. Ando, Phys. Rev. Lett. **90**, 227201 (2003).
[8] A. Maignan, V. Caignaert, B. Raveau, D. Khomskii, and G. Sawatzky, Phys. Rev. Lett. **93**, 026401 (2004).
[9] M. A. Señarís-Rodríguez and J. B. Goodenough, J. Solid State Chem. **116**, 224 (1995).
[10] M. A. Korotin, S. Yu. Ezhov, I. V. Solovyev, V. I. Anisimov, D. I. Khomskii, and G. A. Sawatzky, Phys. Rev. B **54**, 5309 (1996).
[11] C. Zobel, M. Kriener, D. Bruns, J. Baier, M. Grüninger, T. Lorenz, P. Reutler, and A. Revcolevschi, Phys. Rev. B **66**, 020402(R) (2002).
[12] D. P. Kozlenko, N. O. Golosova, Z. Jirák, L. S. Dubrovinsky, B. N. Savenko, M. G. Tucker, Y. Le Godec, and V. P. Glazkov, Phys. Rev. B **75**, 064422 (2007).
[13] K. Knížek, Z. Jirák, J. Hejtmánek, M. Veverka, M. Maryško, G. Maris, and T. T. M. Palstra, Eur. Phys. J. B **47**, 213 (2005).
[14] M. Kriener, C. Zobel, A. Reichl, J. Baier, M. Cwik, K. Berggold, H. Kierspel, O. Zabara, A. Freimuth, and T. Lorenz, Phys. Rev. B **69**, 094417 (2004).
[15] Z. Hu, H. Wu, M. W. Haverkort, H. H. Hsieh, H. J. Lin, T. Lorenz, J. Baier, A. Reichl, I. Bonn, C. Felser, A. Tanaka, C. T. Chen, and L. H. Tjeng, Phys. Rev. Lett. **92**, 207402 (2004).
[16] C. Frontera, J. L. Garcia-Munoz, A. E. Carrillo, M. A. G. Aranda, I. Margiolaki, and A. Caneiro, Phys. Rev. B **74**, 054406 (2006).
[17] D. D. Khalyavin, D. N. Argyriou, U. Amann, A. A. Yaremchenko, and V. V. Kharton, Phys. Rev. B **75**, 134407 (2007).
[18] S. Ya. Istomin, J. Grins, G. Svensson, O. A. Drozhzhin, V. L. Kozhevnikov, E. V. Antipov, and J. P. Attfield, Chem. Mater. **15**, 4012 (2003).
[19] S. Ya. Istomin, O. A. Drozhzhin, G. Svensson, and E. V. Antipov, Solid State Sci. **6**, 539 (2004).
[20] R. L. Withers, M. James, and D. J. Goossens, J. Solid State Chem. **174**, 198 (2003).
[21] D. J. Goossens, K. F. Wilson, M. James, A. J. Studer, and X. L. Wang, Phys. Rev. B **69**, 134411 (2004).
[22] A. Baszczuk, S. Kolesnik, B. Dabrowski, O. Chmaissem, and J. Mais, Phys. Rev. B **76**, 134407 (2007).
[23] F. Lindberg, O. A. Drozhzhin, S. Ya. Istomin, G. Svensson, F. B. Kaynak, P. Svedlindh, P. Warnicke, A. Wannberg, A. Mellergard, and E. V. Antipov, J. Solid State Chem. **179**, 1434 (2006).
[24] A. Maignan, S. Hebert, V. Caignaert, V. Pralong, and D. Pelloquin, J. Solid State Chem. **178**, 868 (2005).
[25] Y. Zhang, S. Sasaki, T. Odagiri, and M. Izumi, Phys. Rev. B **74**, 214429 (2006).
[26] N. A. Dubrovinskaia and L. S. Dubrovinsky, Rev. Sci. Instrum. **74**, 3433 (2003).
[27] A. P. Hammersley, S. O. Svensson, M. Hanfland, A. N. Fitch, and D. Hausermann, High Press. Res. **14**, 235 (1996).
[28] R. B. Von Dreele and A. C. Larson, General Structure Analysis System (GSAS), Los Alamos National Laboratory Report No. LAUR 86-748, 1986 (unpublished).
[29] V. L. Aksenov, A. M. Balagurov, V. P. Glazkov, D. P. Kozlenko, I. V. Naumov, B. N. Savenko, D. V. Sheptyakov, V. A. Somenkov, A. P. Bulkin, V. A. Kudryashev, and V. A. Trounov, Physica B **265**, 258 (1999).
[30] V. P. Glazkov and I. N. Goncharenko, Fiz. Tekh. Vys. Davlenii **1**, 56 (1991) (in Russian).
[31] V. B. Zlokazov and V. V. Chernyshev, J. Appl. Crystallogr. **25**, 447 (1992).
[32] J. Rodríguez-Carvajal, Physica B **192**, 55 (1993).
[33] F. J. Birch, J. Geophys. Res. **91**, 4949 (1986).
[34] N. O. Golosova, D. P. Kozlenko, V. I. Voronin, and B. N. Savenko, Phys. Solid State **48**, 96 (2006).
[35] R. Lengsdorf, M. Ait-Tahar, S. S. Saxena, M. Ellerby, D. I. Khomskii, H. Micklitz, T. Lorenz, and M. M. Abd-Elmeguid, Phys. Rev. B **69**, 140403(R) (2004).
[36] D. V. Sheptyakov, O. A. Drozhzhin, V. Yu. Pomjakushin, S. Ya. Istomin, I. A. Bobrikov, E. V. Antipov, and A. M. Balagurov, FLNP JINR Annual Report (unpublished).